High dynamic range image reconstruction for multi-bit quanta image sensor*

GAO Jing[1], SHANG Zongyao[1], NIE Kaiming[1], and LUO Tao[2]**

1. Tianjin Key Laboratory of Imaging and Sensing Microelectronic Technology, School of Microelectronics, Tianjin University, Tianjin 300072, China

2. College of Intelligence and Computing, Tianjin University, Tianjin 300072, China

(Received 28 January 2022; Revised 21 April 2022)

An adaptive thresholds algorithm is proposed in this letter, which is used to determine the global optimal thresholds for multi-bit quanta image sensor (MB-QIS). Firstly, the senor model of MB-QIS is set up. Then global optimal thresholds theory is analyzed and a thresholds optimization algorithm based on the binary search is designed to determine the optimal global thresholds. Finally, the high dynamic range (HDR) images are reconstructed by the non-iterative maximum likelihood estimation (MLE) image reconstruction method. The results of simulation prove that HDR imaging of MB-QIS is realized by the proposed method effectively.

Document code: A **Article ID:** 1673-1905(2022)09-0553-6

DOI https://doi.org/10.1007/s11801-022-2014-9

In 2005, FOSSUM[1,2] firstly proposed the concept of digital film sensor (DFS), and in 2011, named it quanta image sensor (QIS), which had the advantages of spatial oversampling, time oversampling, and photon counting. Conceptually, the pixels of QIS are sub-diffraction-limit, high conversion gain, and low full-well-capacity. They are called “jots”. Each “jot” can detect a single photon[3]. The output of binary data indicates the numbers of photons are above or below a certain threshold. They are represented as bit cubes and finally processed to reconstruct images. The concept of spatial and temporal accumulation is shown in Fig.1. In 2013, the single-bit QIS (SB-QIS) and multi-bit QIS (MB-QIS) were modeled and analyzed[4]. Each sub-pixel of MB-QIS outputs a multi-bit binary number. Compared to SB-QIS, the linearity or compression of MB-QIS data between average input photon flux and output signal could be adjusted by selecting the bit depth. Besides, the field readout rate and amount of data could be reduced with the bit depth increasing[5,6].

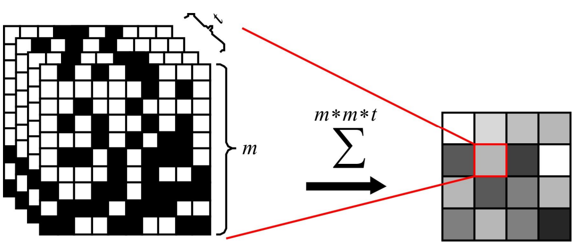

Fig.1 Diagram of spatial and temporal accumulation

Previous work about the model of QIS[7] and methods of image reconstruction[8-12] were analyzed. Several high dynamic range (HDR) imaging methods were designed. Based on non-iterative image reconstruction, an optimal threshold method was given[13], which required that a pixel (or a group of pixels) had an optimal threshold. And an optimized weight HDR reconstruction algorithm with high and low exposure data for QIS was also realized[14]. Besides, denoising of the non-fixed column noise for QIS was analyzed[15]. Two types of QIS were tested in Refs.[16] and [17]. Effect of bit error rate (*BER*), bit depth, quantum efficiency, dark current, and read noise were analyzed[18] and a low noise readout circuit was designed[19]. Threshold offset was resolved by adding a capacitive trans-impedance amplifier (CTIA) before 1-bit analog-to-digital converter (ADC)[20].

In recent years, researches mainly focused on pixels and readout circuits design. Some image processing algorithms applied to QIS were also realized, but researches on HDR algorithms were few. The optimal threshold method[13] was effective, but it was used on SB-QIS, one optimal threshold caused one group of data so that it is slow. As for the HDR algorithm[14], high and low exposure data were required. Without optimal thresholds, its reconstruction quality was low.

In this letter, an adaptive thresholds adjustment method applied to MB-QIS was described. Based on the principle of QIS, the senor model of MB-QIS was set up. Then, the optimal threshold theory for MB-QIS was analyzed and a thresholds optimization algorithm based on binary search was designed. Finally, simulation results were given.

* This work has been supported by the National Key R&D Program of China (No.2019YFB2204300).

** E-mail: luo_tao@tju.edu.cn

The imaging principle of QIS is as follows.

Assuming that the quantum efficiency of jots is 100%, the probability of receiving x photons by one jot in one frame follows a Poisson distribution as

$$P[x] = \frac{\mathrm{e}^{-H} H^{x}}{x!}, \tag{1}$$

where H represents the average number of the received photons.

For the SB-QIS, after being quantified by the threshold of 1-bit ADC, binary data b_m is obtained as

$$b_m = \begin{cases} 1, \text{ if } x \geq q \\ 0, \text{ otherwise} \end{cases}. \tag{2}$$

The threshold q=1 is abstracted mathematically as the quantization threshold corresponding to a photon. The probabilities of states "0" and "1" are

$$P[b_m = 0] = P[x < q] = \sum_{i=0}^{q-1} \frac{\mathrm{e}^{-H} H^{i}}{i!} = \mathrm{e}^{-H}, \tag{3}$$

and

$$P[b_m = 1] = P[x \geq q] = \sum_{i=q}^{\infty} \frac{\mathrm{e}^{-H} H^{i}}{i!} = 1 - \mathrm{e}^{-H}, \tag{4}$$

respectively.

For the k-bit MB-QIS, the average output code value is

$$\bar{x} = \sum_{x=0}^{2^k-1} x \cdot P[x] + \sum_{x=2^k}^{\infty} (2^k - 1) \cdot P[x]. \tag{5}$$

Spatial oversampling is achieved by jots with photon incidence and temporal oversampling is achieved by multiple sampling of high frame rate. According to the Poisson distribution, the light source generates the random number of photons, which are then converted into an electrical signal by jots. The signal is transmitted to the readout circuit by the column bus and then quantized by the k-bit ADC to output binary data. There are a series of binary states. "0" indicates no photon, and "$1-2^{k-1}$" indicates one photon to more. In a continuous light field, t frames are achieved by exposure t times repeatedly.

As shown in Fig.2, the model of QIS is modeled as follows[21].

(1) For the grayscale matrix $\boldsymbol{C}_{n\times n}$, each factor is converted into a matrix of size $m\times m$ by bicubic interpolation. So, matrix $\boldsymbol{C}_{n\times n}$ will be changed into matrix $\boldsymbol{C}_{mn\times mn}$.

(2) To match light intensity, the enlarged matrix $\boldsymbol{C}_{mn\times mn}$ is multiplied by a light intensity coefficient h_0 and the matrix $\boldsymbol{H}_{mn\times mn}$ is got. $\boldsymbol{H}_{mn\times mn}$ is converted to a random number according to a Poisson distribution. This conversion simulates shot noise.

(3) In the quantization process, the output signal containing shot noise is compared to k-bit thresholds Q and binary jot bit is obtained.

(4) Repeat the steps (2) and (3) for t times to generate t frames. The original value of a pixel is converted to an $m\times m\times t$ jot bit cubicle.

(5) The sum of the bit cubicle constitutes the quantitative results $S_{n\times n}$. $S_{n\times n}$ is reconstructed by the non-iterative image reconstruction method to get image[8].

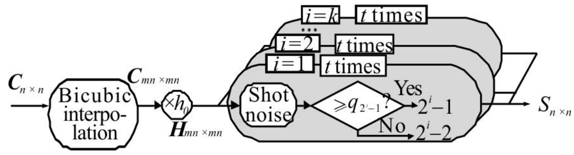

Fig.2 MB-QIS imaging model

In this model, the spatial oversampling rate is m^2, the time oversampling rate is t and the number of bits is k.

In this letter, 4-bit MB-QIS is simulated, the multi-bit thresholds are 1—15, and the oversampling rate of MB-QIS is 4×4×16.

The relationship between signal-to-noise ratio (SNR) and q was given in Ref.[13]. When threshold q made γ= 0.5, SNR was maximum. γ as the bit density, which was defined as

$$\gamma = 1 - \frac{S_{n\times n}}{L}, \tag{6}$$

where $S_{n\times n}$ is the quantitative results, and L is oversampling rate.

According to Poisson distribution, when H=q, γ is nearest to 0.5. The optimal threshold is equal to the number of incident photons.

For SB-QIS, the incident photons are quantified by only one threshold, when the threshold is equal to the number of incident photons, the SNR is the highest. For MB-QIS, the incident photons will be quantified by k-bit thresholds. Due to the shot noise, there is a probability of H quantified by each threshold q_i. The probability follows the Poisson distribution, which is shown in Fig.3.

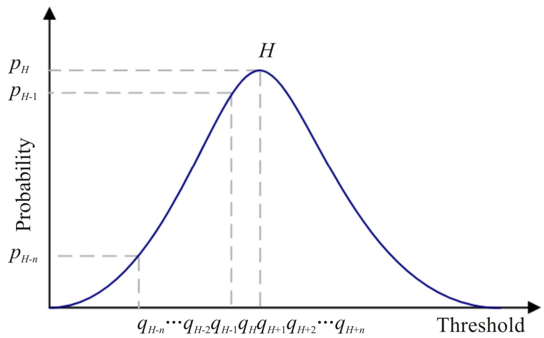

Fig.3 Quantified probabilities of multi-bit thresholds

p_H is the probability that the incident photons H is quantified by the optimal threshold q_H, and the probability of other thresholds can still be calculated. The SNR of MB-QIS for incident photons H can be defined as

$$SNR_{\mathrm{MB}} = \sum_{i=1}^{2^k-1} SNR_i \cdot p_i, \tag{7}$$

where SNR_i is the SNR that the incident photon H quantified by q_i, and p_i is the probability that the incident photon H is quantified by q_i.

To maximize the SNR_{MB}, p_i should be as high as possible. According to the Poisson distribution, the threshold with the highest probability is q_H, and the probabilities of

H quantified by other thresholds gradually decrease from q_H. Therefore, for the number of incident photons H, its optimal multi-bit thresholds are $\{q_H, q_{H\pm1}, q_{H\pm2}, \dots q_{H\pm2^k-1}\}$.

For a group of incident photons $H=[H_1, H_2, H_3, \dots H_{2^k-1}]$, each H_i corresponds to a group of optimal multi-bit thresholds Q_i. For a 4-bit MB-QIS, the probabilities of each H_i quantified by different q_i are shown in Fig.4.

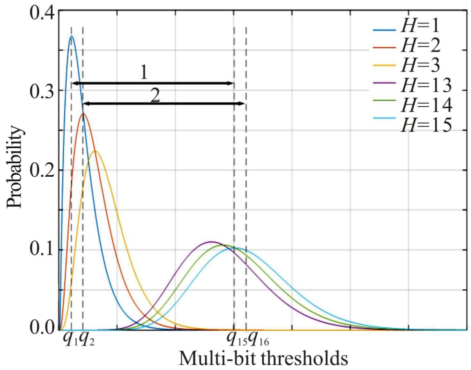

Fig.4 Quantified probabilities of different q_i

Interval 1 in Fig.4 is the optimal multi-bit thresholds Q_8 of H=8, and these thresholds make each H have its optimal single-bit threshold q_i. Interval 2 is the optimal multi-bit thresholds Q_9 of H=9. Compared with 1, there is no optimal single-bit threshold q_1 but q_{16}. However, H=16 does not exist. q_{16} could not get the highest *SNR* without H=16. In other words, the non-optimal *SNR* of q_{16} replaces the optimal *SNR* of q_1. For H=1—15, the global *SNR* of Q_8 is higher than that of Q_9. Similarly, the global *SNR* of Q_8 is higher than that of the other Q_i. For incident photons H=1—15, the global optimal thresholds should be Q_8, whose range matches the number of incident photons. For any k-bit MB-QIS, the conclusion is still applicable. Its global optimal thresholds are the multi-bit thresholds whose upper and lower limits match the upper and lower limits of the number of incident photons.

Define the probability P_{M_i} as

$$P_{M_i}=\frac{M_i}{2^k-1}, \tag{8}$$

where M_i is the number of the same thresholds between the global thresholds and the optimal multi-bit thresholds Q_i. So, the global *SNR* could be defined as

$$SNR_{\mathrm{MBg}}=\sum_{i=1}^{2^k-1} SNR_{\mathrm{MB}i}\cdot P_{M_i}. \tag{9}$$

As we can see, to make SNR_{MBg} the highest, each P_{M_i} should be the highest. The global optimal thresholds should include q_i of the optimal multi-bit thresholds Q_i as many as possible. Obviously, the global optimal thresholds analyzed before could make SNR_{MBg} the highest.

Fig.5 shows the global *SNR* of incident photons H=8—22 with different optimal multi-bit thresholds Q_i (i=8—22). In theory, the global optimal thresholds are Q_{15}. And the global *SNR* of Q_{15} is also the highest.

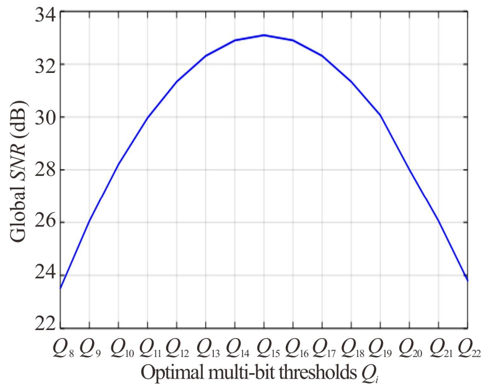

Fig.5 Global *SNR* with different Q_i

Considering the maximum and the minimum numbers of incident photons, the bit density is shown in Fig.6.

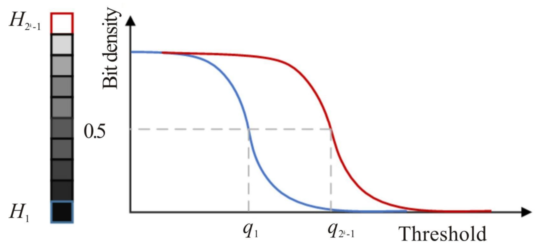

(a) Bit density of the maximum and the minimum numbers of incident photons

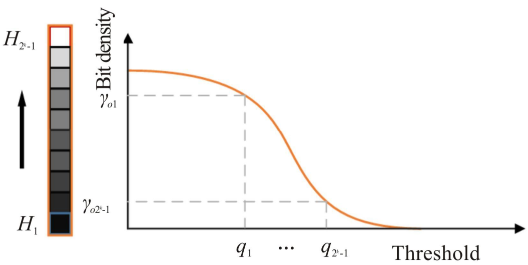

(b) Bit density of all the incident photons

Fig.6 Bit density of different thresholds

In Fig.6(a), the bit density of the maximum and the minimum numbers of incident photons with the optimal thresholds are shown. Based on the analysis above, the optimal thresholds are q_1=H_1 and $q_{2^k-1}=H_{2^k-1}$. The range of the global optimal thresholds should be q_1 to q_{2^k-1}. Fig.6(b) shows the bit density of all the incident photons with the global thresholds whose range is q_1 to q_{2^k-1}.

The optimal bit density γ_o is defined as

$$\gamma_\mathrm{o}=1-\frac{S_\mathrm{o}}{(2^k-1)\times L}=1-\frac{\bar{x}_\mathrm{o}}{2^k-1}, \tag{10}$$

where $\bar{x}_\mathrm{o}$ is the optimal output code value. Substituting

H_i=q_i into Eq.(5), $\overline{x}_{\mathrm{o}}$ could be got. S_{o} is the optimal value of quantitative results, which is

$$S_{\mathrm{o}} = L \times \overline{x}_{\mathrm{o}}, \tag{11}$$

where L is the oversample rate.

In Fig.6(b), $\gamma_{\mathrm{o}1}$ and $\gamma_{\mathrm{o}2^k-1}$ are the optimal bit density of q_1 and q_{2^k-1}. As long as the upper and lower limits of the bit density are $\gamma_{\mathrm{o}2^k-1}$ and $\gamma_{\mathrm{o}1}$, the quantization results are kept as the optimal value S_{o}. So, the global optimal threshold could be determined.

During the adjustment process, if multi-bit thresholds deviate from linear, the quantitative results will be incorrect. To keep the multi-bit thresholds as linear as possible, the proposed method adjusts as follows. Determine the increased value of the maximum threshold q_{2^k-1} (minimum threshold q_1) is determined at first, if it needs to be increased by 1, the maximum threshold q_{2^k-1} (minimum threshold q_1) is increased by 1; if it needs to be increased by 2, the maximum threshold (minimum threshold q_1) is increased by 2 and q_{2^k-1} (q_2) is increased by 1. If the maximum threshold q_{2^k-1} by σ, then σ numbers of thresholds need to be increased. The process is as shown in Eq.(12). The maximum threshold q_{2^k-1} is increased by σ, q_{2^k-2} is increased by σ−1, and so on, until $q_{2^k-\sigma}$ is increased by 1. The procedure for minimum threshold adjustment is the same.

$$\begin{aligned} q_{2^k-1} &= q_{2^k-1} + \sigma, \\ q_{2^k-2} &= q_{2^k-2} + \sigma - 1, \\ q_{2^k-3} &= q_{2^k-3} + \sigma - 2, \\ &\cdots \\ q_{2^k-\sigma} &= q_{2^k-\sigma} + 1, \end{aligned} \tag{12}$$

where σ is set at first, which is

$$\sigma = q_{\mathrm{M}2^k-1} / 2^{n-1}, \tag{13}$$

where n is the number of iterations, k is the number of bits, $q_{\mathrm{M}2^k-1}$ is the maximum threshold of Q_{M}, Q_{M} is the multi-bit thresholds after each iteration. Before the first iteration, Q_{M}=Q.

By increasing $q_{\mathrm{M}2^k-1}$ as Eq.(12), there will be two situations as follows.

(1) Maximum quantitative result $S_{\mathrm{M}2^k-1}$ is in the error tolerance of the optimal value $S_{\mathrm{o}2^k-1}$. The upper limit of the global optimal thresholds is determined.

(2) Maximum quantitative result $S_{\mathrm{M}2^k-1}$ is lower than the optimal value $S_{\mathrm{o}2^k-1}$. A binary search is used to determine the upper limit. Binary search interval [q_a, q_b] is

$$q_a = q_{\mathrm{M}2^k-1(n-1)}, \tag{14}$$

$$q_b = q_{\mathrm{M}2^k-1(n)}, \tag{15}$$

where n is the number of the last iteration before binary search.

During the binary search, $q^{n-1}_{\mathrm{M}2^k-1}$ is increased as Eq.(12), σ= q_m− $q^{n-1}_{\mathrm{M}2^k-1}$, q_m is

$$q_m = \lceil (q_a + q_b)/2 \rceil. \tag{16}$$

If $S_{\mathrm{M}2^k-1}$ is lower than $S_{\mathrm{o}2^k-1}$, q_b is made equal to q_m; if $S_{\mathrm{M}2^k-1}$ is higher than $S_{\mathrm{o}2^k-1}$, q_a is made equal to q_m.

For q_1, binary search is also used. When the minimum quantitative result is lower than the optimal value $S_{\mathrm{o}1}$, the lower limit was not adjusted, because if the input is lower than 1, the minimum quantitative result is always lower than the optimal value $S_{\mathrm{o}1}$.

The binary search interval is dependent on step length. In this letter, the step length of MB-QIS is 1, binary search interval [q_a, q_b] is

$$q_a = q_1, \tag{17}$$

$$q_b = q_{2^k-1} - 2^k + 1, \tag{18}$$

where q_1 and q_{2^k-1} belong to Q, whose upper limit has been determined.

After the upper limit and the lower limit are determined, the global optimal thresholds could be got. Algorithm is as followed.

Tab.1 Multi-bit thresholds update scheme

Algorithm
Initial S_{2^k-1} is more (or less) than $S_{\mathrm{o}2^k-1}$
Set Q_{M}=Q, compute $S_{\mathrm{M}2^k-1}$ and $S_{\mathrm{o}2^k-1}$
while $\lvert S_{\mathrm{M}2^k-1} - S_{\mathrm{o}2^k-1} \rvert > e$ **do**, where e is error,
compute σ_n
if $\lvert S_{\mathrm{M}2^k-1} - S_{\mathrm{o}2^k-1} \rvert > e$, update Q_{M}, compute $S_{\mathrm{M}2^k-1}$ and $S_{\mathrm{o}2^k-1}$
if $\lvert S_{\mathrm{M}2^k-1} - S_{\mathrm{o}2^k-1} \rvert < -e$,
while $\lvert S_{\mathrm{M}2^k-1} - S_{\mathrm{o}2^k-1} \rvert > e$ **do**,
compute $q_m = \lceil (q_a + q_b)/2 \rceil$, $S_{\mathrm{M}2^k-1}$ and $S_{\mathrm{o}2^k-1}$, where $\lceil \cdot \rceil$ is ceiling operator.
if $\lvert S_{\mathrm{M}2^k-1} - S_{\mathrm{o}2^k-1} \rvert < -e$, then set q_b=q_m,
else, set q_a=q_m.
end while
end while
return *Q*
Initial S_1 is more than $S_{\mathrm{o}1}$
compute $q_m = \lceil (q_a + q_b)/2 \rceil$, and $S_{\mathrm{o}1}$, where $\lceil \cdot \rceil$ is ceiling operator.
while $\lvert S_{\mathrm{M}1} - S_{\mathrm{o}1} \rvert > e$, **do**
if $S_{\mathrm{M}1} - S_{\mathrm{o}1} < -e$, then set q_b=q_m,
else, set q_a=q_m.
compute $q_m = \lceil (q_a + q_b)/2 \rceil$, $S_{\mathrm{M}1}$ and $S_{\mathrm{o}1}$
end while
return *Q*

To prove the validity of the proposed method, images "Castle" and "Giraffe" were used for simulation. The images quality after reconstruction was evaluated and analyzed subjectively and objectively. Peak-signal-to-noise-ratio (*PSNR*) and structural similarity (*SSIM*) were used to evaluate the reconstructed image.

In Fig.7, the results of different images are shown, which are different images and different numbers of photons. The maximum number of incident photons of “Castle” is 30, “Giraffe” is 30 and 45. *PSNR* and *SSIM* are shown in Tab.2.

(a) “Castle” with the initial thresholds (b) “Castle” with the proposed method

(c) “Giraffe” with the initial thresholds (d) “Giraffe” with the proposed method

(e) “Giraffe” (45) with the initial thresholds (f) “Giraffe” (45) with the proposed method

Fig.7 Comparison of different scenes

Tab.2 Comparison of objective indicators

	Image with initial threshold		Image with adaptive threshold	
	PSNR	*SSIM*	*PSNR*	*SIMM*
Castle	23.796 3	0.772 5	26.893 5	0.885 5
Giraffe	22.675 6	0.586 4	31.331 9	0.844 0
Giraffe(45)	17.637 7	0.664 6	31.291 2	0.847 2

The comparison with the methods in Refs.[13] and [14] is shown in Fig.8. The maximum number of incident photons of “Castle” and “Giraffe” is 30.

The run time is represented by the number of iterations. *PSNR*, *SSIM*, and iterations are shown in Tab.3.

Compared with the method in Ref.[13], the iterations of the proposed method are fewer, because the proposed method only determines two thresholds. The method in Ref.[13] makes a pixel (or a group of pixels) have its own optimal threshold in Ref.[13]. This causes a large number of iterations and sampling frames.

(a) “Castle” with the initial threshold (b) “Castle” with the proposed method

(c) “Castle” with Ref.[13] (d) “Castle” with Ref.[14]

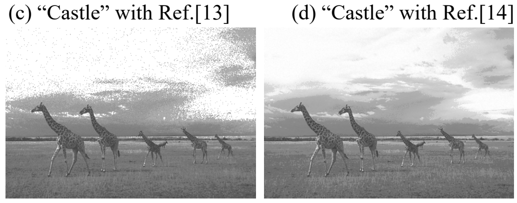

(e) “Giraffe” with the initial threshold (f) “Giraffe” with the proposed method

(g) “Giraffe” with Ref.[13] (h) “Giraffe” with Ref.[14]

Fig.8 Comparison of different methods

Tab.3 Comparison of optimal threshold method and the proposed method

Method	Castle			Giraffe		
	PSNR	*SSIM*	Iterations	*PSNR*	*SSIM*	Iterations
Proposed	26.893 5	0.885 5	10	31.331 9	0.844 0	12
Ref.[13]	26.846 8	0.899 7	122	31.721 9	0.889 1	125
Ref.[14]	24.460 4	0.858 6	14	28.927 8	0.839 2	11

Compared with the method in Ref.[14], the quality of reconstruction results of the proposed method is higher, because the high and low exposure data is got by initial thresholds. Quantitative results are not optimal, so the quality of reconstruction results is lower.

In conclusion, an adaptive threshold algorithm for MB-QIS was proposed. The proposed method improved the dynamic range by determining global optimal thresholds. Experiment results show that the proposed method could effectively improve dynamic range in different scenes with few iterations and the quality of reconstruction results is high.

Statements and Declarations

The authors declare that there are no conflicts of interest related to this article.

References

[1] FOSSUM E R. What to do with sub-diffraction-limit (SDL) pixels?- a proposal for a gigapixel digital film sensor (DFS)[C]//IEEE Workshop on Charge-Coupled Devices and Advanced Image Sensors, 2005, Nagano, Japan. New York：IEEE, 2005：214-217.

[2] FOSSUM E R. The quanta image sensor (QIS)：concepts and challenges[C]//Imaging Systems and Applications, July 10-14, 2011, Toronto, Canada. Washington：Optical Society of America, 2011：10-14.

[3] MASOODIAN S, MA J, STARKEY D, et al. A 1Mjot 1040fps 0.22e-rms stacked BSI quanta image sensor with cluster-parallel readout[C]//2017 International Image Sensor Workshop, May 30-June 2, 2017, Hiroshima, Japan. International Image Sensor Society, 2017：230-233.

[4] FOSSUM E R. Modeling the performance of single-bit and multi-bit quanta image sensors[J]. IEEE journal of the electron devices society, 2013, 1(9)：166-174.

[5] FOSSUM E R. Multi-bit quanta image sensors[C]//2015 International Image Sensor Workshop, June 8-11, 2015, Vaals, The Netherlands. International Image Sensor Society, 2015：292-295.

[6] YIN Z Y, WANG Y B M, FOSSUM E R. Low bit-depth ADCs for multi-bit quanta image sensors[J]. IEEE journal of solid-state circuits, 2021, 56(3)：950-960.

[7] YANG F, LU Y M, SBAIZ L, et al. Bits from photons：oversampled image acquisition using binary Poisson statistics[J]. IEEE transactions on image processing, 2012, 21(4)：1421-1436.

[8] CHAN S H, ELGENDY O A, WANG X. Images from bits：non-iterative image reconstruction for quanta image sensors[J]. Sensors, 2016, 16(11)：1961-1982.

[9] ROJAS R A, LUO W Y, MURRAY V, et al. Learning optimal parameters for binary sensing image reconstruction algorithms[C]//2017 IEEE International Conference on Image Processing, September 17-20, 2017, Beijing, China. New York：IEEE, 2017：2791-2795.

[10] CHOI J H, ELGENDY O A, CHAN S H. Image reconstruction for quanta image sensors using deep neural networks[C]//2018 IEEE International Conference on Acoustics, Speech and Signal Processing, April 15-20, 2018, Calgary, AB, Canada. New York：IEEE, 2018：6543-6547.

[11] CHAN S H, LU Y M. Efficient image reconstruction for gigapixel quantum image sensors[C]//Proceedings of the 2014 IEEE Global Conference on Signal and Information Processing, December 3-5, 2014, Atlanta, GA USA. New York：IEEE, 2014：312-316.

[12] WONG H T, LEUNG C S, HO D. Theoretical analysis and image reconstruction for multi-bit quanta image sensors[J]. Signal processing, 2021, 185：108087.

[13] ELGENDY O A, CHAN S H. Optimal threshold design for quanta image sensor[J]. IEEE transactions on computational imaging, 2017, 4(1)：99-111.

[14] GNANASAMBANDAM A, MA J, CHAN S H. HDR imaging with quanta image sensors：theoretical limits and optimal reconstruction[J]. IEEE transactions on computational imaging, 2020, 6：1571-1585.

[15] GAO J, DU X X, NIE K M, et al. Analysis and elimination method of the non-fixed column noise for quantum image sensor[J]. IEEE sensor journal, 2020, 20(1)：318-327.

[16] MA J J, ZHANG D X, ELGENDY O A, et al. A 0.19e-rms read noise 16.7Mpixel stacked quanta image sensor with 1.1 μm-pitch backside illuminated pixels[J]. IEEE electron device letters, 2021, 42(6)：891-894.

[17] MA J J, ZHANG D X, ELGENDY O A, et al. A photon-counting 4Mpixel stacked BSI quanta image sensor with 0.3e-read noise and 100dB single-exposure dynamic range[C]//2021 Symposium on VLSI Technology, June 13-19, 2021, Kyoto, Japan. New York：IEEE, 2021.

[18] LIU B W, XU J T. Modeling the photon counting and photoelectron counting characteristics of quanta image sensors[J]. Journal of semiconductors, 2021, 42(6)：062301.

[19] ZHAO T, GAO J, XU J T, et al. Optimized oversampling and readout circuit design for quanta image sensor[J]. Laser & optoelectronics progress, 2021, 58(24)：2403001. (in Chinese)

[20] FOSSUM E R. Analog read noise and quantizer threshold estimation from quanta image sensor bit density[J]. IEEE journal of the electron devices society, 2022, 10：269-274.

[21] XU J T, ZHAO X Y, HAN L Q, et al. Effect of the transition points mismatch on quanta image sensors[J]. Sensors, 2018, 18(12)：4357-4370.